

# MOTChallenge 2015: Towards a Benchmark for Multi-Target Tracking

Laura Leal-Taixé\*, Anton Milan\*, Ian Reid, Stefan Roth, and Konrad Schindler

**Abstract**—In the recent past, the computer vision community has developed centralized benchmarks for the performance evaluation of a variety of tasks, including generic object and pedestrian detection, 3D reconstruction, optical flow, single-object short-term tracking, and stereo estimation. Despite potential pitfalls of such benchmarks, they have proved to be extremely helpful to advance the state of the art in the respective area. Interestingly, there has been rather limited work on the standardization of quantitative benchmarks for multiple target tracking. One of the few exceptions is the well-known PETS dataset [20], targeted primarily at surveillance applications. Despite being widely used, it is often applied inconsistently, for example involving using different subsets of the available data, different ways of training the models, or differing evaluation scripts. This paper describes our work toward a novel multiple object tracking benchmark aimed to address such issues. We discuss the challenges of creating such a framework, collecting existing and new data, gathering state-of-the-art methods to be tested on the datasets, and finally creating a unified evaluation system. With *MOTChallenge* we aim to pave the way toward a unified evaluation framework for a more meaningful quantification of multi-target tracking.

**Index Terms**—multiple people tracking, benchmark, evaluation metrics, dataset



## 1 INTRODUCTION

Evaluating and comparing multi-target tracking methods is not trivial for numerous reasons (*cf. e.g.* [37]). First, unlike for other tasks, such as image denoising, the ground truth, *i.e.* the perfect solution one aims to achieve, is difficult to define clearly. Partially visible, occluded, or cropped targets, reflections in mirrors or windows, and objects that very closely resemble targets all impose intrinsic ambiguities, such that even humans may not agree on one particular ideal solution. Second, a number of different evaluation metrics with free parameters and ambiguous definitions often lead to inconsistent quantitative results across the literature. Finally, the lack of pre-defined test and training data makes it difficult to compare different methods fairly.

Multi-target tracking is a crucial problem in scene understanding, which, in contrast to other research areas, still lacks large-scale benchmarks. We believe that a unified evaluation platform that allows participants to submit not only their own tracking methods, but also their own data, including video and annotations, as well as propose new evaluation methodologies that can be applied instantaneously to all previous approaches, can bring a vast benefit to the computer vision community.

To that end we develop the *MOTChallenge* benchmark, consisting of three main components: (1) a publicly avail-

able dataset, (2) a centralized evaluation method, and (3) an infrastructure that allows for crowdsourcing of new data, new evaluation methods and even new annotations. The first release of the dataset contains a total of 22 sequences, half for training and half for testing, with a total of 11286 frames or 996 seconds of video. Camera calibration is provided for 4 of those sequences to enable 3D real-world coordinate tracking. We also provide pre-computed object detections, annotations, and a common evaluation method for all datasets, so that all results can be compared in a fair way. The final goal is to collect sequences from all researchers who are willing to contribute to the benchmark, enabling an update of the data, new evaluation tools, new annotations, etc. to be made available yearly.

We anticipate two ways of submitting to the *MOTChallenge* benchmark: (1) year-round, or (2) submissions to a specific workshop or challenge, which is to be held once a year. The purpose of the former is to keep track of state-of-the-art methods submitted at major conferences and journals, to allow for a fair comparison between methods by ensuring that all are using the same datasets and the same evaluation methods. The latter follows the well-known format of yearly challenges that have been very successful in other areas, *e.g.*, in the PASCAL VOC series [19] or the ImageNet competitions [42]. These challenges and workshops provide a way to track and discuss the progress and innovations of state-of-the-art methods presented over the year. The first workshop [2] organized on the *MOTChallenge* benchmark took place in early 2015 in conjunction with the Winter Conference on Applications of Computer Vision (WACV).

\* = authors contributed equally.

L. Leal-Taixé\* and K. Schindler are with the Photogrammetry and Remote Sensing Group at ETH Zurich, Switzerland.

A. Milan\* and I. Reid are with the Australian Centre for Visual Technologies at the University of Adelaide, Australia.

S. Roth is with the Department of Computer Science, Technische Universität Darmstadt, Germany.

Primary contacts: leal@geod.baug.ethz.ch, anton.milan@adelaide.edu.au

**Goals.** This paper has three main goals:

- 1) To discuss the challenges of creating a multi-object tracking benchmark;
- 2) to analyze current datasets and evaluation methods;
- 3) to bring forward the strengths and weaknesses of state-of-the-art multi-target tracking methods.

The benchmark with all datasets, current ranking and submission guidelines can be found at:

<http://www.motchallenge.net/>

## 1.1 Related work

**Benchmarks and challenges.** In the recent past, the computer vision community has developed centralized benchmarks for numerous tasks including object detection [19], pedestrian detection [17], 3D reconstruction [45], optical flow [9], [22], visual odometry [22], single-object short-term tracking [28], and stereo estimation [22], [43]. Despite potential pitfalls of such benchmarks (e.g. [48]), they have proved to be extremely helpful to advance the state of the art in the respective area. For multiple target tracking, in contrast, there has been very limited work on standardizing quantitative evaluation.

One of the few exceptions is the well known PETS dataset [20], targeted primarily at surveillance applications. The 2009 version consisted of 3 subsets, S1 targeted at person count and density estimation, S2 targeted at people tracking, and S3 targeted at flow analysis and event recognition. The easiest sequence for tracking (S2L1) consisted of a scene with few pedestrians, and for that sequence state-of-the-art methods perform extremely well with accuracies of over 90% given a good set of initial detections [24], [36], [55]. Methods then moved to tracking on the hardest of the sequences (with most crowd density), but hardly ever on the complete dataset. Even for this widely used benchmark, we observe that tracking results are commonly obtained in an inconsistent fashion: involving using different subsets of the available data, different detection inputs, inconsistent model training that is often prone to overfitting, and varying evaluation scripts. Results are thus not easily comparable. So the question that arises here is: Are these sequences already too easy for current tracking methods, are methods simply overfitted, or are they poorly evaluated?

The PETS team organized a workshop approximately once a year to which researchers could submit their results, and methods were evaluated under the same conditions. Although this was indeed a fair comparison, the fact that submission was only once a year meant that the use of this benchmark for high impact conferences like ICCV or CVPR still remained an issue.

A well-established and useful way of organizing datasets is through standardized challenges. These are usually in the form of web servers that host the data and through which results are uploaded by the users. Results

are then computed in a centralized way by the server and afterwards presented online to the public, making comparison with any other method immediately possible. There are several datasets organized in this fashion: the Labeled Faces in the Wild [25] for unconstrained face recognition, the PASCAL VOC [19] for object detection, the ImageNet large scale visual recognition challenge [42], or the Reconstruction Meets Recognition Challenge (RMRC) [1].

Recently, the KITTI benchmark [22] was introduced for challenges in autonomous driving, which included stereo/flow, odometry, road and lane estimation, object detection and orientation estimation, as well as tracking. Some of the sequences include crowded pedestrian crossings, making the dataset quite challenging, but the camera position is always the same for all sequences (at a car’s height).

With the *MOTChallenge* benchmark, we aim to increase the difficulty by including a variety of sequences filmed from different viewpoints, with different lighting conditions, and different levels of crowd density. In addition to other existing and new data, we include sequences from both PETS and KITTI datasets. The real challenge we see is not to perform well on an individual sequence, but rather to perform well on a diverse set of sequences.

Another work that is worth mentioning is [4], in which the authors collect a very large amount of data with 42 million pedestrian trajectories. Since annotation of such a large collection of data is infeasible, they use a denser set of cameras to create the “ground truth” trajectories. Though we do not aim at collecting such a large amount of data, the goal of our benchmark is somewhat similar: to push research in tracking forward by generalizing the test data to a larger set that is highly variable and hard to overfit.

**Evaluation.** A critical point with any dataset is how to measure the performance of the algorithms. In the case of multiple object tracking, the CLEAR metrics [27] have emerged as one of the standard measures. By measuring the intersection over union of bounding boxes and matching those from annotations and results, measures of accuracy and precision can be computed. Precision measures how well the persons are localized, while accuracy evaluates how many distinct errors such as missed targets, ghost trajectories, or identity switches are made.

Another set of measures that is widely used in the tracking community is that of [33]. There are three widely used metrics introduced in that work: mostly tracked, mostly lost, and partially tracked pedestrians. These numbers give a very good intuition on the performance of the method. We refer the reader to Section 5 for more formal definitions.

A key parameter in the both families of metrics is the intersection-over-union threshold, which determines if a bounding box is matched to an annotation or not. It is fairly common to observe methods compared under

different thresholds, varying from 25% to 50%. There are often many other variables and implementation details that differ between evaluation scripts, but which may affect results significantly.

It is therefore clear that standardized benchmarks are the only way to compare methods in a fair and principled way. Using the same ground truth data and evaluation methodology is the only way to guarantee that the only part being evaluated is the tracking method that delivers the results. This is the main goal behind this paper and behind the *MOTChallenge* benchmark.

## 2 BENCHMARK SUBMISSION

Our benchmark consists of the database and evaluation server on one hand, and the website as the user interface on the other. It is open to everyone who respects the submission policies (see next section). Before participating, every user is required to create an account, if possible providing an institutional and not a generic e-mail address<sup>1</sup>. After registering, the user can create a new tracker with a unique name and enter all additional details. It is mandatory to indicate

- the challenge or benchmark category in which the tracker will be participating,
- the full name and a brief description of the method including the parameters used,
- whether the method operates online or on a batch of frames and whether the source code is publicly available,
- the *total* runtime in seconds for computing the results on all sequences and the hardware used, and
- whether only the provided or also external training and detection data were used.

After entering all details, it is possible to submit the results in the format described in Sec. 3.4. The tracking results will be automatically evaluated and appear on the user's profile. They will *not* be displayed in the public ranking table. The user can then decide at any point in time to make the results public. Note that the results can be published anonymously, *e.g.* to enable a blind review process for a corresponding paper. In this case, we ask to provide the venue and the paper ID or a similar unique reference. We request that a proper reference to the method's description is added upon acceptance of the paper. In case of rejection, an anonymous entry may also be removed from the database. Anonymous entries will also be removed after six months of inactivity.

The tracker's meta information such as description, or project page can be edited at any time. Visual results of all public submissions, as well as annotations and detections can be viewed on a dedicated visualization page<sup>2</sup>.

1. For accountability and to prevent abuse by using several email accounts.

2. <http://motchallenge.net/vis/>

### 2.1 Submission policy

The main goal of this benchmark is to provide a platform that allows for an objective performance comparison of multiple target tracking approaches on real-world data. Therefore, we introduce a few simple guidelines that must be followed by all participants.

**Training.** Ground truth is only provided for the training sequences. It is the participant's own responsibility to find the best setting using *only* the training data. The use of additional training data must be indicated during submission and will be visible in the public ranking table. The use of ground truth labels on the test data is strictly forbidden. This or any other misuse of the benchmark will lead to the deletion of the participant's account and their results.

**Detections.** We also provide a unique set of detections (see Sec. 3.3) for each sequence. We expect all tracking-by-detection algorithms to use the given detections. In case the user wants to present results with another set of detections or is not using detections at all, this should be clearly stated during submission and will also be displayed in the results table.

**Submission frequency.** Generally, we expect one single submission for every tracking approach. If for any reason, the user needs to re-compute and re-submit the results (*e.g.* due to a bug discovered in the implementation), he/she may do so after a waiting period of 72 hours after the last submission. This policy should discourage the use of the benchmark server for training and parameter tuning on the test data. The number of submissions is counted and displayed for each method. Under *no* circumstances must anyone create a second account and attempt to re-submit in order to bypass the waiting period. This may lead to a deletion of the account and excluding the user from participating in the benchmark.

### 2.2 Challenges

Besides the main benchmarks (2D MOT 2015, 3D MOT 2015), we anticipate to organize multi-target tracking challenges on a regular basis, similar in spirit to the widely known PASCAL VOC series [19], or the ImageNet competitions [42]. The main differences to the main benchmark are:

- The dataset is typically smaller, but potentially more challenging.
- There is a fixed submission deadline for all participants.
- The results are revealed and the winners awarded at a corresponding workshop.

The first edition of our series was the WACV 2015 Challenge that consisted of six new outdoor sequences with both moving and static cameras. The results were presented at the BMTT Workshop [2] held in conjunction with WACV 2015.

Training sequences											
Name	FPS	Resolution	Length	Tracks	Boxes	Density	3D	Camera	Viewpoint	Shadows	Source
TUD-Stadtmitte	25	640x480	179 (00:07)	10	1156	6.5	yes	static	medium	cloudy	[5]
TUD-Campus	25	640x480	71 (00:03)	8	359	5.1	no	static	medium	cloudy	[6]
PETS09-S2L1	7	768x576	795 (01:54)	19	4476	5.6	yes	static	high	cloudy	[20]
ETH-Bahnhof	14	640x480	1000 (01:11)	171	5415	5.4	yes	moving	low	cloudy	[18]
ETH-Sunnyday	14	640x480	354 (00:25)	30	1858	5.2	yes	moving	low	sunny	[18]
ETH-Pedcross2	14	640x480	840 (01:00)	133	6263	7.5	no	moving	low	sunny	[18]
ADL-Rundle-6	30	1920x1080	525 (00:18)	24	5009	9.5	no	static	low	cloudy	new
ADL-Rundle-8	30	1920x1080	654 (00:22)	28	6783	10.4	no	moving	medium	night	new
KITTI-13	10	1242x375	340 (00:34)	42	762	2.2	no	moving	medium	sunny	[22]
KITTI-17	10	1242x370	145 (00:15)	9	683	4.7	no	static	medium	sunny	[22]
Venice-2	30	1920x1080	600 (00:20)	26	7141	11.9	no	static	medium	sunny	new
<b>Total training</b>			<b>5503 (06:29)</b>	<b>500</b>	<b>39905</b>	<b>7.3</b>					

Testing sequences											
Name	FPS	Resolution	Length	Tracks	Boxes	Density	3D	Camera	Viewpoint	Weather	Source
TUD-Crossing	25	640x480	201 (00:08)	13	1102	5.5	no	static	medium	cloudy	[6]
PETS09-S2L2	7	768x576	436 (01:02)	42	9641	22.1	yes	static	high	cloudy	[20]
ETH-Jelmoli	14	640x480	440 (00:31)	45	2537	5.8	yes	moving	low	sunny	[18]
ETH-Linthescher	14	640x480	1194 (01:25)	197	8930	7.5	yes	moving	low	sunny	[18]
ETH-Crossing	14	640x480	219 (00:16)	26	1003	4.6	no	moving	low	cloudy	[18]
AVG-TownCentre	2.5	1920x1080	450 (03:45)	226	7148	15.9	yes	static	high	cloudy	[10]
ADL-Rundle-1	30	1920x1080	500 (00:17)	32	9306	18.6	no	moving	medium	sunny	new
ADL-Rundle-3	30	1920x1080	625 (00:21)	44	10166	16.3	no	static	medium	sunny	new
KITTI-16	10	1242x370	209 (00:21)	17	1701	8.1	no	static	medium	sunny	[22]
KITTI-19	10	1242x374	1059 (01:46)	62	5343	5.0	no	moving	medium	sunny	[22]
Venice-1	30	1920x1080	450 (00:15)	17	4563	10.1	no	static	medium	sunny	new
<b>Total testing</b>			<b>5783 (10:07)</b>	<b>721</b>	<b>61440</b>	<b>10.6</b>					

TABLE 1: Overview of the sequences currently included in the benchmark.

### 3 DATASETS

One of the key aspects of any benchmark is data collection. The goal of *MOTChallenge* is not only to compile yet another dataset with completely new data, but rather to: (1) create a common framework to test tracking methods on; (2) gather existing and new challenging sequences with very different characteristics (frame rate, pedestrian density, illumination or point of view) in order to challenge researchers to develop more general tracking methods that can deal with all types of sequences. In Table 1 we show an overview of the sequences included in the benchmark.

#### 3.1 2D MOT 2015 sequences

We have compiled a total of 22 sequences, of which we use half for training and half for testing. The annotations of the testing sequences will not be released in order to avoid (over)fitting of the methods to the specific sequences. Nonetheless, the test data contains over 10 minutes of footage and 61440 annotated bounding boxes, therefore, it is hard for algorithms to overfit on such a large amount of data. This is one of the major strengths of the benchmark.

Sequences are very different from each other, we can classify them according to:

- Moving or static camera: the camera can be held by a person [2], placed on a stroller [18] or on a car [22], or can be positioned fixed in the scene.

- Viewpoint: the camera can overlook the scene from a high position, a medium position (at pedestrian’s height), or at a low position.
- Weather: the weather conditions in which the sequence was taken are reported in order to get an estimate of the illumination conditions of the scene. Sunny sequences may contain shadows and saturated parts of the image, while the night sequence contains a lot of motion blur, making pedestrian detection and tracking rather challenging. Cloudy sequences on the other hand contain fewer of those artifacts.

We divided the sequences into training and testing in order to have a balanced distribution, as we can see in Figure 1.

##### 3.1.1 New sequences

We introduce 6 new challenging sequences, 4 filmed from a static camera and 2 from a moving camera held at pedestrian’s height. Three of the sequences are particularly difficult: a night sequence filmed from a moving camera and two outdoor sequences with a high density of pedestrians. The moving camera together with the low illumination creates a lot of motion blur, making this sequence extremely challenging. In the future, we will include further sequences captured on rainy or foggy days and evaluate how methods perform under those special conditions. A special challenge including only these 6 new sequences was held at the 1st Workshop on Benchmarking Multi-Target Tracking [2]. The best per-

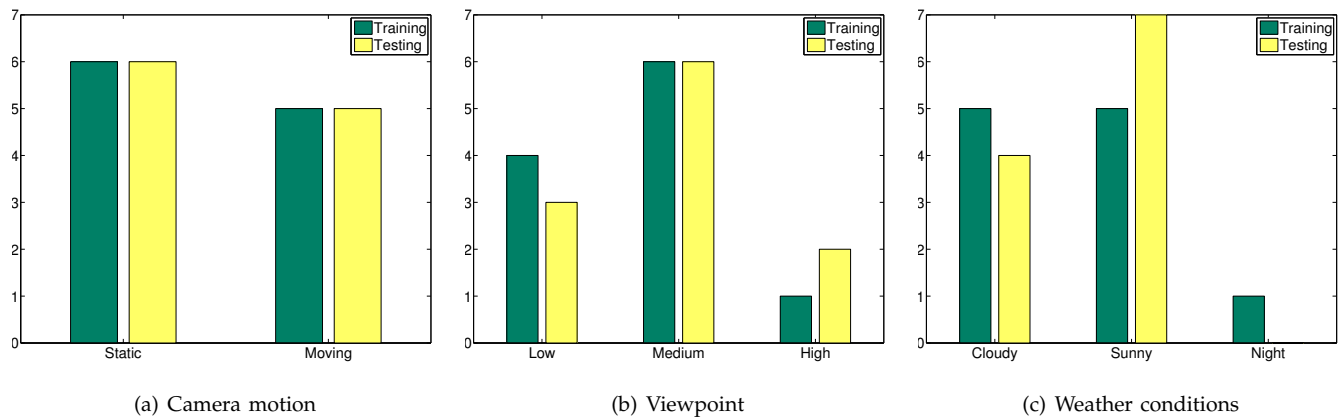


Fig. 1: Comparison histogram between training and testing sequences of (a) static vs. moving camera, (b) camera viewpoint: low, medium or high, (c) weather conditions: cloudy, sunny, or night.

forming algorithm reached a MOTA (tracking accuracy) of 12.7%, showing how challenging these new sequences are<sup>3</sup>.

### 3.2 3D MOT 2015 sequences

A pedestrian’s 3D position is typically obtained by projecting the 2D position of the feet of the person into the 3D world, *e.g.*, by using a homography between the image plane and the ground plane. The bottom-center point of the bounding box is commonly chosen to represent the position of the feet of the pedestrian, but this may not be particularly accurate, if the bounding box is not placed very tightly around the pedestrian’s silhouette, or if the limbs are extended asymmetrically. By the nature of projective geometry, even slight 2D misplacements can cause large 3D errors. It is therefore clear, that obtaining accurate 3D information only from bounding boxes is a challenging task.

In this section, we detail how the 3D information is obtained for both static and moving cameras, and discuss whether current calibration and annotation pairs are accurate enough for reliable 3D tracking. For the sequences with a moving camera we show that these errors are too large for tracking purposes, and therefore we argue not to include those sequences in the 3D benchmark. We thus limit the 3D category to a few available 3D sequences with a static camera, but plan to extend the number of 3D sequences in the near future.

#### 3.2.1 Static camera sequences

For the 4 sequences filmed using a static camera, AVG-TownCentre, PETS09-S2L1, PETS09-S2L2 and TUD-Stadtmitte, the calibration files from the sources [5], [10], [20] are used to compute a 2D homography between the image plane and the ground plane. All  $z$  coordinates are set to 0, indicating the position of the feet of the pedestrian. In order to measure the accuracy of the calibration

for each sequence, we use the manually annotated trajectories and plot the velocities of the pedestrians at each frame. Realistic walking speeds range from 0 – 3 m/s, with a mean comfortable walking speed of 1.4 m/s. This is confirmed by the distribution that we see in Fig. 2(a). The other sequences (Figs. 2(b)-2(d)) have a few speeds in the range of 3 – 10 m/s. These are not real speeds, since there are no running pedestrians in the sequences. These outliers are largely due to projective geometry. For example, variations in the size of the bounding box can introduce artificial shifts in 2D that greatly affect the 3D position in the scene.

The bottom row of Fig. 2 shows the mean speeds per pedestrian and sequence. As we can see, most pedestrians walk at a speed between 1 – 1.5 m/s, hence we can conclude that the calibration is accurate enough for tracking.

We can further analyze the spurious high speeds that we observe in some sequences by plotting a speed distribution in image space as shown in the top row of Fig. 3. For PETS09-S2L2, we can see that most artifacts are concentrated on the bottom-right part of the image, where pedestrians leave the scene. The fact that a leaving pedestrian is cropped by the image border makes the bounding box around it thinner (following the annotation policy of PETS). Since the bottom-center of the bounding box is the 2D position used to obtain the 3D information, the 2D position is likely shifted away from the real position of the pedestrian’s feet. In the case of AVG-TownCentre, we can see some points on the image where unusually high speeds are observed. These are typically far away from the camera and present at the beginning or the end of the sequence, where correct annotation is difficult. This also accounts for the peaks of mean speed in Fig. 4(g), which belong to two pedestrians observed for 2 frames and are far away from the camera. Their position fluctuation is a simple artifact of variability in the bounding box placement. Finally, for the TUD-Stadtmitte sequence, we clearly see that high velocities are concentrated in the part of the image

3. The challenge results are available at [http://motchallenge.net/results/WACV\\_2015\\_Challenge/](http://motchallenge.net/results/WACV_2015_Challenge/).

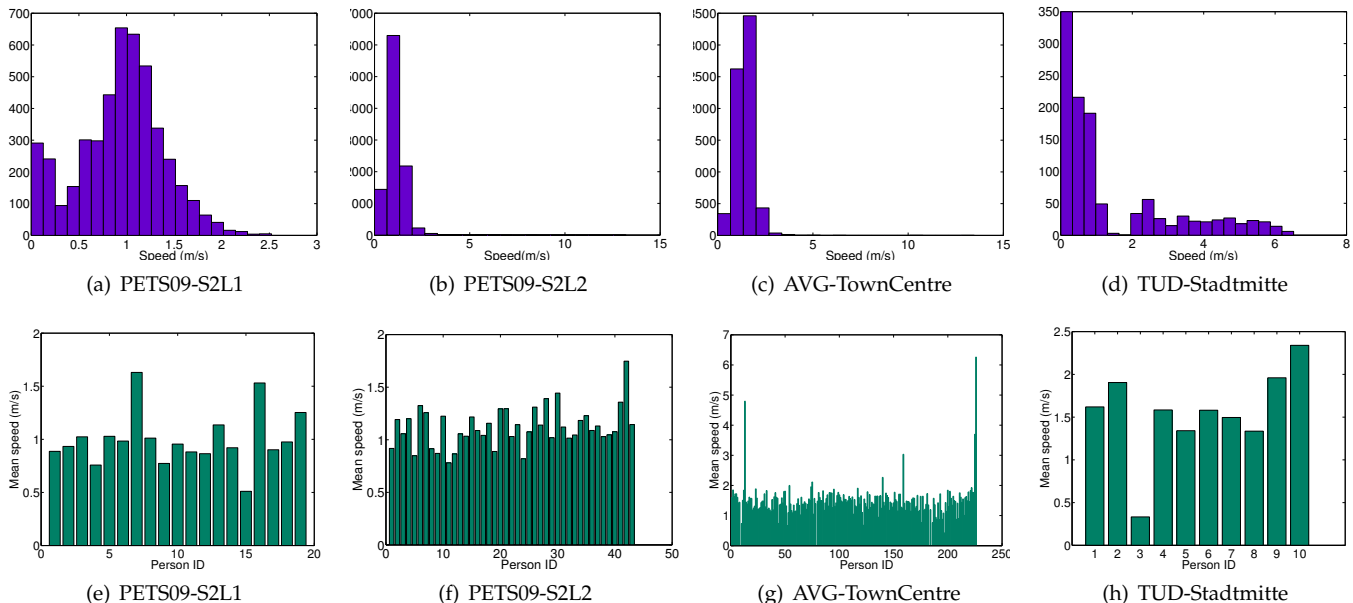


Fig. 2: *Top row*: Pedestrian speed histograms per sequence. *Bottom row*: Mean speed per pedestrian per sequence.

that is far away from the camera, and therefore also far away from the points used for calibration. The bounding box shifts in that area have a bigger impact on the 3D position. Avoiding the effects discussed would require new “3D aware” annotations for each sequence, which we leave for future work.

### 3.2.2 Moving camera sequences

For the sequences with moving cameras, the authors [18] provide one file for each image, containing the calibration of the left camera, which allows us to backproject the feet of the person to the world coordinate system and to find the 3D position by intersecting the ray with the estimated ground plane. The error of this calibration increases significantly as pedestrians move away from the camera, which makes tracking of far away objects very imprecise.

We do the same velocity analysis for these sequences, shown in Fig. 4, and observe that some of the velocities reach 200 – 700 m/s, indicating a clear problem in the 3D position estimation. Looking at the mean velocity per pedestrian, we can observe very high velocities, especially for ETH-Bahnhof and ETH-Linthescher sequences. These are mostly pedestrians walking far away from the camera and usually visible for a short period of time. This is further observable in the maps of Fig. 5, where we can see that these incorrect peak velocities are found mostly in the region far away ( $\sim 10$  m) from the camera. This again illustrates the challenge of obtaining accurate 3D information from 2D bounding boxes, simply due to the nature of projective geometry. For these sequences, the added inaccuracy introduced by the automatic ground plane angle estimation makes the 3D information unreliable, which is why we decided not to include these sequences in the 3D benchmark.

As future work, we plan on using the additional view provided for these sequences to strengthen the 3D estimation. Ideally and for all sequences, the pedestrian’s feet should be annotated directly, since in general annotations for 2D and 3D tracking purposes may differ. Further annotation issues are discussed in Sec. 5.1.

### 3.3 Detections

To detect pedestrians in all images, we use the recent object detector implementation of Dollár *et al.* [16], which is based on aggregated channel features (ACF). We rely on the default parameters and the pedestrian model trained on the INRIA dataset [14], rescaled with a factor of 0.6 to enable the detection of smaller pedestrians. The minimal bounding box height in our benchmark is 59 pixels. The detector performance along with three sample frames is depicted in Fig. 6 for both the training and the test set of the benchmark. Note that the recall does not reach 100% because of the non-maximum suppression applied.

Obviously, we cannot (nor necessarily want to) prevent anyone from using a different set of detections, or even rely on a different set of features altogether. However, we require that this is noted as part of the tracker’s description and is also displayed in the ratings table.

### 3.4 Data format

All images were converted to JPEG and named sequentially to a 6-digit file name (*e.g.* 000001.jpg). Detection and annotation files are simple comma-separated value (CSV) files. Each line represents one object instance, and it contains 10 values as shown in Tab. 2.

The first number indicates in which frame the object appears, while the second number identifies that object

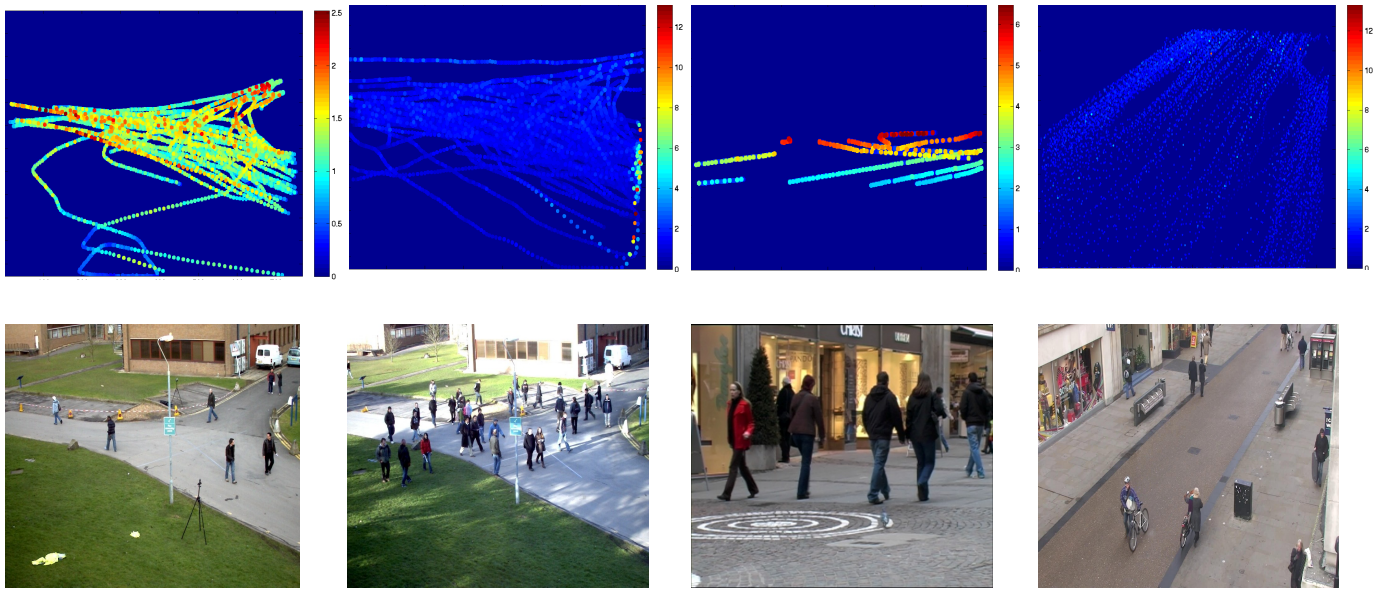


Fig. 3: *Top row*: Speed distributions in image space for the PETS09-S2L1, PETS09-S2L2, AVG-TownCentre and TUD-Stadtmitte sequences, respectively. Note that the scale is different for each image. *Bottom row*: Sample frame for each sequence.

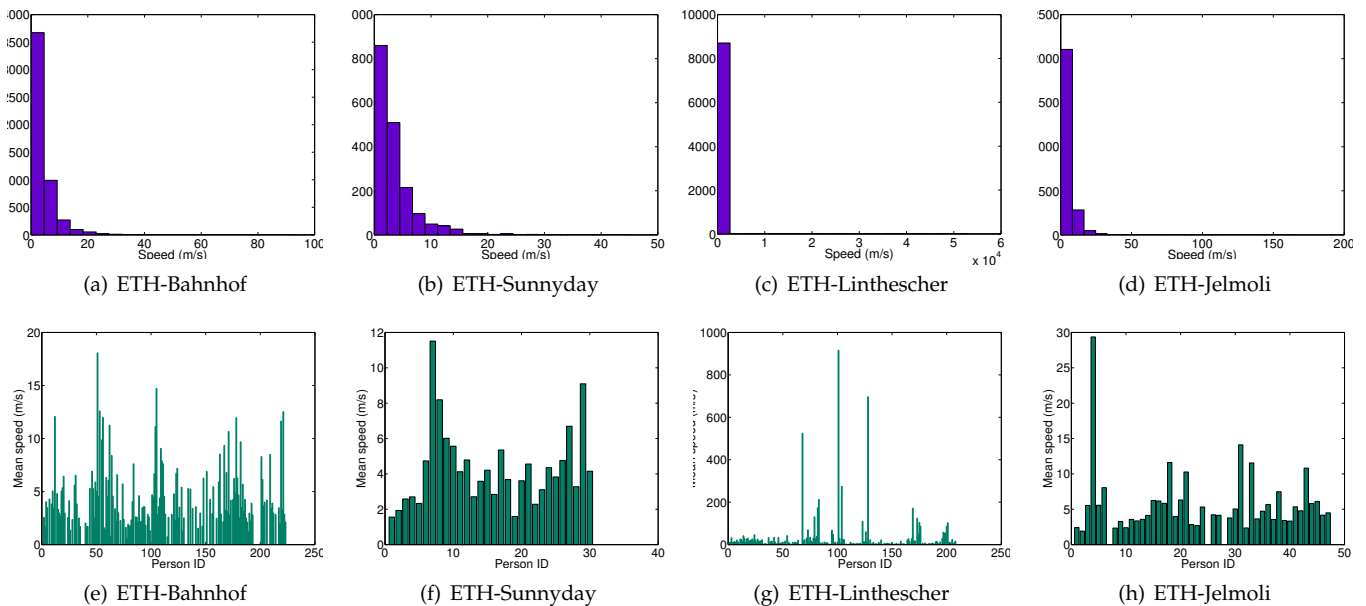


Fig. 4: *Top row*: Pedestrian speed histograms per sequence. *Bottom row*: Mean speed per pedestrian per sequence.

as belonging to a trajectory by assigning a unique ID (set to  $-1$  in a detection file, as no ID is assigned yet). Each object can be assigned to only one trajectory. The next four numbers indicate the position of the bounding box of the pedestrian in 2D image coordinates. The position is indicated by the top-left corner as well as width and height of the bounding box. This is followed by a single number, which in case of detections denotes their confidence score. The last three numbers indicate the 3D position in real-world coordinates of the pedestrian. This position represents the feet of the person. In the case of 2D tracking, these values will be ignored and can be left

at  $-1$ .

An example of such a detection 2D file is:

```
1, -1, 794.2, 47.5, 71.2, 174.8, 67.5, -1, -1, -1
1, -1, 164.1, 19.6, 66.5, 163.2, 29.4, -1, -1, -1
1, -1, 875.4, 39.9, 25.3, 145.0, 19.6, -1, -1, -1
2, -1, 781.7, 25.1, 69.2, 170.2, 58.1, -1, -1, -1
```

For the ground truth and results files, the 7<sup>th</sup> value (confidence score) acts as a flag whether the entry is to be considered. A value of 0 means that this particular instance is ignored in the evaluation, while a value of 1 is used to mark it as active.

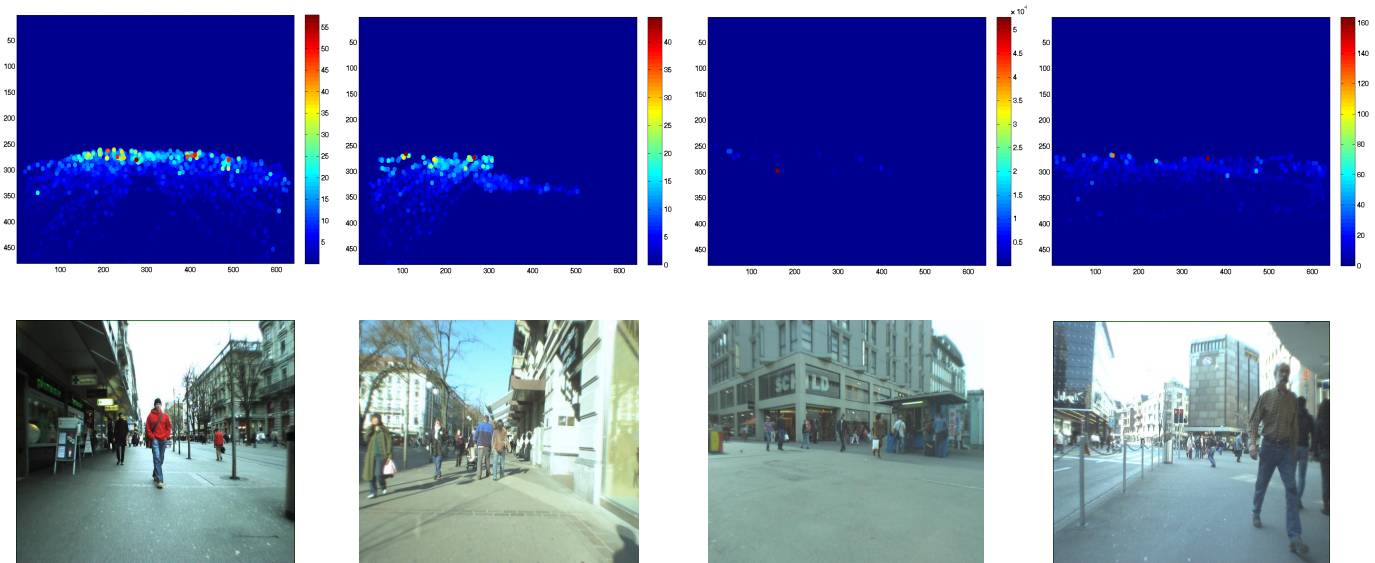


Fig. 5: *Top row*: Speed distributions in image space for the ETH-Bahnhof, ETH-Sunnyday, ETH-Linthescher and ETH-Jelmoli sequences, respectively. Note that the scale is different for each image. *Bottom row*: Sample frame for each sequence.

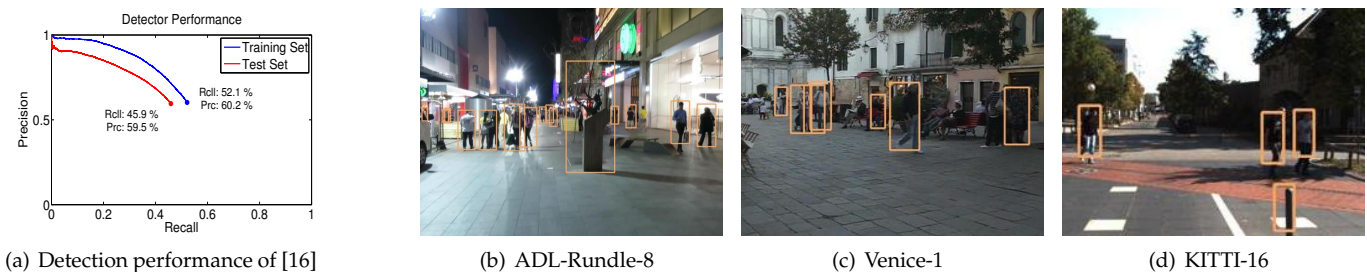


Fig. 6: (a) The performance of the provided detection bounding boxes evaluated on the training (blue) and the test (red) set. The circle indicates the operating point (*i.e.* the input detection set) for the trackers. (b-d) Exemplar detection results.

An example of such an annotation 2D file is:

```
1, 1, 794.2, 47.5, 71.2, 174.8, 1, -1, -1, -1
1, 2, 164.1, 19.6, 66.5, 163.2, 1, -1, -1, -1
1, 3, 875.4, 39.9, 25.3, 35.0, 0, -1, -1, -1
2, 1, 781.7, 25.1, 69.2, 170.2, 1, -1, -1, -1
```

In this case, there are 2 pedestrians in the first frame of the sequence, with identity tags 1, 2. The third pedestrian is too small and therefore not considered, which is indicated with a flag value (7<sup>th</sup> value) of 0. In the second frame, we can see that pedestrian 1 remains in the scene. Note, that since this is a 2D annotation file, the 3D positions of the pedestrians are ignored and therefore are set to -1. Note that all values including the bounding box are 1-based, *i.e.* the top left corner corresponds to (1, 1).

To obtain a valid result for the entire benchmark, a separate CSV file following the format described above must be created for each sequence and called ```Sequence-Name.txt```. All files must be compressed into a single zip file that can then be uploaded to be evaluated.

### 3.5 Expansion through crowdsourcing

We foresee a yearly update of the benchmark datasets in order to include new, more challenging sequences and eventually remove outdated or repetitive sequences. The goal is to push forward research in multi-target tracking by increasing the difficulty of the data as new, more accurate methods are proposed by the community. We want to make a call to the community to share their sequences, detections or annotations to the benchmark, so as to include a large variety of data. More importantly, the goal is to increase the type of data to the following categories:

- Tracking of cars, bicycles, etc. in outdoor scenarios;
- Biological data such as cell, bird or fish tracking;
- Sports data: basketball games, hockey or soccer;
- Large-scale multi-view sequences.

Sequences of such scenarios do exist in the literature, *e.g.* thousands of bats filmed using thermal cameras [53], cell tracking data [32], basketball game [11], hockey



Position	Name	Description
1	Frame number	Indicate at which frame the object is present
2	Identity number	Each pedestrian trajectory is identified by a unique ID (−1 for detections)
3	Bounding box left	Coordinate of the top-left corner of the pedestrian bounding box
4	Bounding box top	Coordinate of the top-left corner of the pedestrian bounding box
5	Bounding box width	Width in pixels of the pedestrian bounding box
6	Bounding box height	Height in pixels of the pedestrian bounding box
7	Confidence score	Indicates how confident the detector is that this instance is a pedestrian. For the ground truth and results, it acts as a flag whether the entry is to be considered.
8	$x$	3D $x$ position of the pedestrian in real-world coordinates (−1 if not available)
9	$y$	3D $y$ position of the pedestrian in real-world coordinates (−1 if not available)
10	$z$	3D $z$ position of the pedestrian in real-world coordinates (−1 if not available)

TABLE 2: Data format for the input and output files, both for detection and annotation files.

game [38], several indoor multi-view sequences [11], or recent large-scale multi-view sequences containing millions of pedestrian trajectories [4]. We encourage the community to contact us with any interesting data that they would like included in the benchmark structure, and we commit to extending the benchmark to other interesting and relevant categories. Each category will have its own separate submissions.

## 4 BASELINE METHODS

As a starting point for the benchmark, we have included a number of recent multi-target tracking approaches as baselines, which we will briefly outline for completeness but refer the reader to the respective publication for more details. Note that we have used the publicly available code and trained all of them in the same way<sup>4</sup> (*cf.* Sec. 4.1). However, we explicitly state that the provided numbers may not represent the best possible performance for each method, as could be achieved by the authors themselves. Table 3 lists current benchmark results for all baselines as well as for all anonymous entries at the time of writing of this manuscript.

### 4.1 Training and testing

Most of the available tracking approaches do not include a learning (or training) algorithm to determine the set of model parameters for a particular dataset. Therefore, we follow a simplistic search scheme for all baseline methods to find a good setting for our benchmark. To that end, we take the default parameter set  $\Theta := \{\theta_1, \dots, \theta_P\}$  as suggested by the authors, where  $P$  is the number of free parameters for each method. We then perform 100 independent runs on the training set with varying parameters. In each run, a parameter value  $\theta_i$  is uniformly sampled around its default value in the range  $[\frac{1}{2}\theta_i, 2\theta_i]$ . Finally, the parameter set  $\Theta^*$  that achieved the highest MOTA score across all 100 runs (*cf.* Sec. 5.2.3) is taken as the optimal setting and run once on the test set. The optimal parameter set is stated in the description entry for each baseline method on the benchmark website.

4. Except for TBD, which does not disclose any obvious free parameters.

### 4.2 DP\_NMS: Network flow tracking

Since its original publication [57], a large number of methods that are based on the network flow formulation have appeared in the literature [13], [31], [34], [41], [50]. The basic idea is to model the tracking as a graph, where each node represents a detection and each edge represents a transition between two detections. Special source and sink nodes allow spawning and absorbing trajectories. A solution is obtained by finding the minimum cost flow in the graph. Multiple assignments and track splitting is prevented by introducing binary and linear constraints.

Here we use two solvers: (i) the successive shortest paths approach [41] that employs dynamic programming with non-maxima suppression, termed DP\_NMS; (ii) a linear programming solver that we use for both 2D and 3D data (LP2D and LP3D, respectively), and that appears as a baseline in [29]. This solver uses the Gurobi Library [3].

### 4.3 CEM: Continuous energy minimization

CEM [36] formulates the problem in terms of a high-dimensional continuous energy. Here, we use the basic approach [7] without explicit occlusion reasoning or appearance model. The target state  $\mathbf{X}$  is represented by continuous  $x, y$  coordinates in *all* frames. The energy  $E(\mathbf{X})$  is made up of several components, including a data term to keep the solution close to the observed data (detections), a dynamic model to smooth the trajectories, an exclusion term to avoid collisions, a persistence term to reduce track fragmentations, and a regularizer. The resulting energy is highly non-convex and is minimized in an alternating fashion using conjugate gradient descent and deterministic jump moves.

### 4.4 SMOT: Similar moving objects

The Similar Multi-Object Tracking (SMOT) approach [15] specifically targets situations where target appearance is ambiguous and rather concentrates on using the motion as a primary cue for data association. Tracklets with similar motion are linked to longer trajectories using the generalized linear assignment (GLA) formulation. The motion similarity and the underlying dynamics of a tracklet are modeled as the order of a linear regressor approximating that tracklet.

#### 4.5 TBD: Tracking-by-detection

This two-stage tracking-by-detection (TBD) approach [21], [56] is part of a larger traffic scene understanding framework and employs a rather simple data association technique. The first stage links overlapping detections with similar appearance in successive frames into tracklets. The second stage aims to bridge occlusions of up to 20 frames. Both stages employ the Hungarian algorithm to optimally solve the matching problem. Note that we did not re-train this baseline but rather used the original implementation and parameters provided.

#### 4.6 SFM: Social forces for tracking

Most tracking systems work with the assumption that the motion model for each target is independent, but in reality, a pedestrian follows a series of social rules, *i.e.* is subject to social forces according to other moving targets around him/her. These have been defined in what is called the social force model (SFM) [23], [26] and have recently been applied to multiple people tracking. For the 3D benchmark we include two baselines that include a few hand-designed force terms, such as *collision avoidance* or *group attraction*. The first method (KALMANSFM) [40] includes those in an online predictive Kalman filter approach while the second (LPSFM) [30] includes the social forces in a Linear Programming framework as described in Sec. 4.2. For the 2D benchmark, we include a recent algorithm (MOTICON) [29], which learns an image-based motion context that encodes the pedestrian’s reaction to the environment, *i.e.*, other moving objects. The motion context, created from low-level image features, leads to a much richer representation of the physical interactions between targets compared to hand-specified social force models. This allows for a more accurate prediction of the future position of each pedestrian in image space, information that is then included in a Linear Programming framework for multi-target tracking.

#### 4.7 TC\_ODAL: Tracklet confidence

Robust Online Multi-Object Tracking based on Tracklet Confidence and Online Discriminative Appearance Learning, or TC\_ODAL [8], is the only online method among the baselines. It proceeds in two stages. First, close detections are linked to form a set of short, reliable tracklets. This so-called local association allows one to progressively aggregate confident tracklets. In case of occlusions or missed detections, the tracklet confidence value is decreased and a global association is employed to bridge longer occlusion gaps. Both association techniques are formulated as bipartite matching and tackled with the Hungarian algorithm.

Another prominent component of TC\_ODAL is online appearance learning. To that end, positive samples are collected from tracklets with high confidence and incremental linear discriminant analysis (ILDA) is employed to update the appearance model in an online fashion.

## 5 EVALUATION

Evaluating multiple object tracking to this day remains a surprisingly difficult task. Even though many measures have been proposed in the past [12], [33], [44], [46], [47], [52], comparing a new method against prior art is typically not straightforward. As discussed in some of our previous work [37], the reasons for that are diverse ranging from ambiguous ground truth, imprecise metric definitions or implementation variations. In this section we will describe the entire evaluation procedure of our benchmark in detail.

### 5.1 Annotations

As in many other applications, multi-target tracking requires a set of labeled (or annotated) videos in order to quantitatively evaluate the performance of a particular approach. Unfortunately, human supervision is necessary to obtain a reliable set of this, so-called ground truth. Depending on factors like object count, image quality, or the level-of-detail, annotating video data can be a rather tedious task. This is one of the reasons why there exist only relatively few datasets with publicly available ground truth.

For the majority of the sequences contained in our benchmark, we employ the publicly available ground truth. The 6 new sequences (*ADL-Rundle-\** and *Venice-\**) were annotated by us using the VATIC annotation tool [49]. We provide the ground truth for the training set, however, to reduce overfitting on unseen data, the annotations for the test sequences are withheld. Annotation samples are illustrated in Fig. 7.

#### 5.1.1 Variation in the annotations

Publicly available annotations contain a relatively large amount of variation. Since, as of now, we rely on different sources for our annotations, we cannot state that they all follow a set of common rules. Some bounding boxes enclose the whole pedestrian, including all the limbs, which can lead to bounding boxes that change noticeably in size depending on the pedestrian’s pose, as we can see in Fig. 8(a), blue pedestrian *vs.* yellow pedestrian. In Fig. 8(b), we see that bounding boxes are not always centered exactly on the pedestrians, which could cause small shifts in the 3D position estimation. Another common problem is that bounding boxes for pedestrians that are close to the camera are usually very tight around the pedestrian’s silhouette compared to pedestrians far away, as we can see in Fig. 8(c), blue bounding box *vs.* yellow bounding box. Occlusions are also handled differently among sequences. While some annotations follow pedestrians even under full occlusion [20], others create a new trajectory once the pedestrian reappears [18].

Recently, a thorough study on face detection benchmarks [35] also showed that annotation policies vary greatly among sequences and datasets. It also showed that adapting the evaluation method to be more robust

Method	AvgRank	MOTA	MOTP	FAR	MT(%)	ML(%)	FP	FN	IDsw	rel.ID	FM	rel.FM	Hz	Ref.
<b>2D MOT 2015</b>														
MOTICON	9.3	23.1 $\pm 16.4$	70.9	1.8	4.7	52.0	10404	35844	1018	24.4	1061	25.5	1.4	[29]
LP2D	8.3	19.8 $\pm 14.2$	71.2	2.0	6.7	41.2	11580	36045	1649	39.9	1712	41.4	112.1	baseline
CEM	9.2	19.3 $\pm 17.5$	70.7	2.5	8.5	46.5	14180	34591	813	18.6	1023	23.4	1.1	[36]
RMOT	10.6	18.6 $\pm 17.5$	69.6	2.2	5.3	53.3	12473	36835	684	17.1	1282	32.0	7.9	[54]
SMOT	10.7	18.2 $\pm 10.3$	71.2	1.5	2.8	54.8	8780	40310	1148	33.4	2132	62.0	2.7	[15]
TBD	12.3	15.9 $\pm 17.6$	70.9	2.6	6.4	47.9	14943	34777	1939	44.7	1963	45.2	0.7	[21], [56]
TC_ODAL	12.8	15.1 $\pm 15.0$	70.5	2.2	3.2	55.8	12970	38538	637	17.1	1716	46.0	1.7	[8]
DP_NMS	10.7	14.5 $\pm 13.9$	70.8	2.3	6.0	40.8	13171	34814	4537	104.7	3090	71.3	444.8	[41]
<b>3D MOT 2015</b>														
LPSFM	1.7	35.9 $\pm 06.3$	54.0	2.3	13.8	21.6	2031	8206	520	10.2	601	11.8	8.4	[30]
LP3D	2.0	35.9 $\pm 11.1$	53.3	4.0	20.9	16.4	3588	6593	580	9.6	659	10.9	83.5	baseline
KALMANFSM	2.3	25.0 $\pm 08.5$	53.6	3.6	6.7	14.6	3161	7599	1838	33.6	1686	30.8	30.6	[39]

TABLE 3: Quantitative results on all baselines.

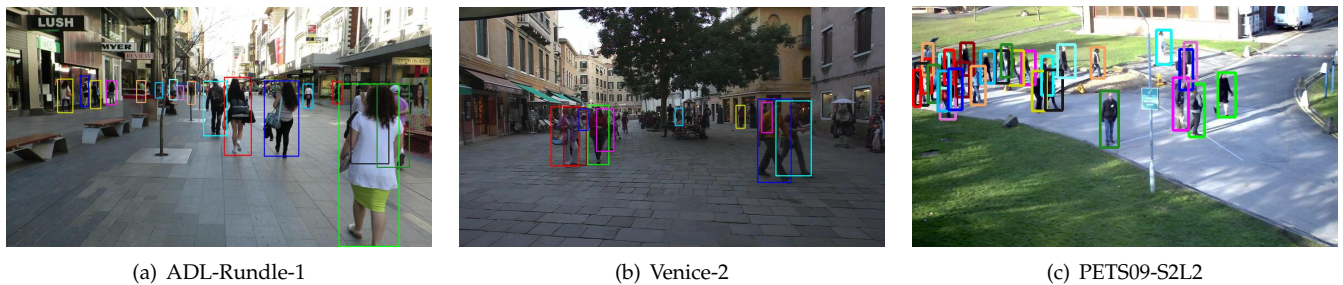


Fig. 7: Ground truth (manually annotated) bounding boxes on three sequences.

against annotation variation plus reannotation of the data with a fixed set of rules changed the performance of many state-of-the-art methods.

Even though annotations based on a standardized policy are not available in the benchmark yet, the larger size and stronger variation in the benchmark already exceed existing benchmarks significantly. Nonetheless, and following the work in [35], we commit to standardizing the set of annotations for all sequences following a common strict set of rules. These annotations will be published in the second release of the benchmark.

## 5.2 Evaluation metrics

In the past, a large number of metrics for quantitative evaluation of multiple target tracking have been proposed [12], [33], [44], [46], [47], [52]. Choosing “the right” one is largely application dependent and the quest for a unique, general evaluation metric is still ongoing. On the one hand, it is desirable to summarize the performance into one single number to enable a direct comparison. On the other hand, one might not want to lose information about the individual errors made by the algorithms and provide several performance estimates, which precludes a clear ranking.

Following the recent trend [8], [36], [51] we employ two sets of measures that have established themselves in the literature: The *CLEAR* metrics proposed by Stiefelhagen *et al.* [47], and a set of track quality measures introduced by Wu and Nevatia [52]. The evaluation

scripts used in our benchmark are publicly available.<sup>5</sup>

### 5.2.1 Tracker-to-target assignment

There are two common prerequisites for quantifying the performance of a tracker. One is to determine for each hypothesized output, whether it is a true positive (TP) that describes an actual (annotated) target, or whether the output is a false alarm (or false positive, FP). This decision is typically made by thresholding based on a defined distance (or dissimilarity) measure  $d$  (see Sec. 5.2.2). A target that is missed by any hypothesis is a false negative (FN). A good result is expected to have as few FPs and FNs as possible. Next to the absolute numbers, we also show the false positive ratio measured by the number of false alarms per frame (FAF), sometimes also referred to as false positives per image (FPPI) in the object detection literature.

Obviously, it may happen that the same target is covered by multiple outputs. The second prerequisite before computing the numbers is then to establish the correspondence between all annotated and hypothesized objects under the constraint that a true object should be recovered at most once, and that one hypothesis cannot account for more than one target.

For the following, we assume that each ground truth trajectory has one unique start and one unique end point, *i.e.* that it is not fragmented. Note that the current evaluation procedure does not explicitly handle target re-identification. In other words, when a target leaves

5. <http://motchallenge.net/devkit>

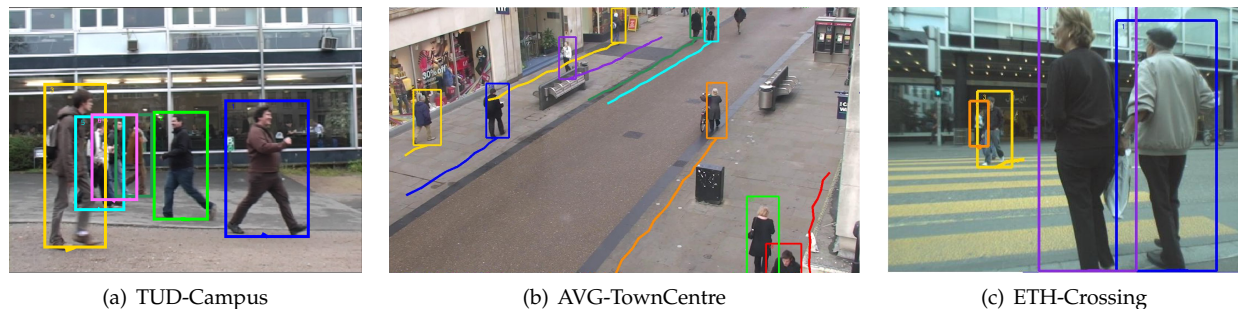


Fig. 8: Publicly available ground truth bounding boxes on three sequences.

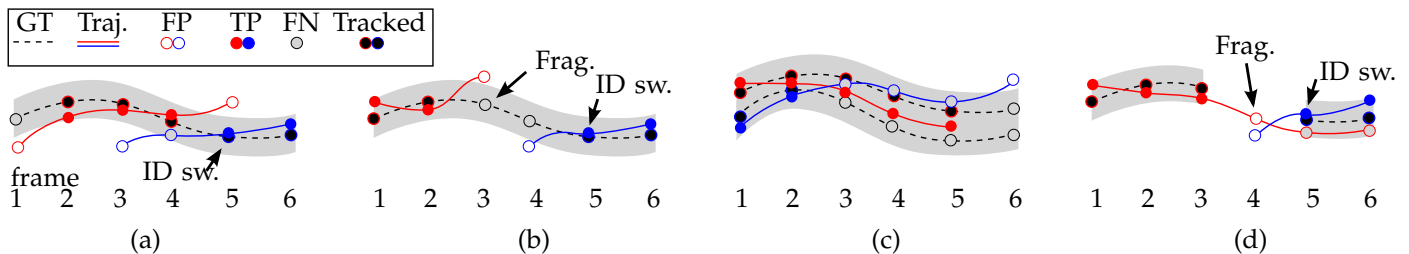


Fig. 9: Four cases illustrating tracker-to-target assignments. (a) An ID switch occurs when the mapping switches from the previously assigned red track to the blue one. (b) A track fragmentation is counted in frame 3 because the target is tracked in frames 1-2, then interrupts, and then reacquires its ‘tracked’ status at a later point. A new (blue) track hypothesis also causes an ID switch at this point. (c) Although the tracking results is reasonably good, an optimal single-frame assignment in frame 1 is propagated through the sequence, causing 5 missed targets (FN) and 4 false positives (FP). Note that no fragmentations are counted in frames 3 and 6 because tracking of those targets is not resumed at a later point. (d) A degenerate case illustrating that target re-identification is not handled correctly. An interrupted ground truth trajectory will typically cause a fragmentation. Also note the less intuitive ID switch, which is counted because blue is the closest target in frame 5 that is not in conflict with the mapping in frame 4.

the field-of-view and then reappears, it is treated as an unseen target with a new ID. As proposed in [47], the optimal matching is found using Munkre’s (a.k.a. Hungarian) algorithm. However, dealing with video data, this matching is not performed independently for each frame, but rather considering a temporal correspondence. More precisely, if a ground truth object  $i$  is matched to hypothesis  $j$  at time  $t - 1$  and the distance (or dissimilarity) between  $i$  and  $j$  in frame  $t$  is below  $t_d$ , then the correspondence between  $i$  and  $j$  is carried over to frame  $t$  even if there exists another hypothesis that is closer to the actual target. A mismatch error (or equivalently an identity switch, IDSW) is counted if a ground truth target  $i$  is matched to track  $j$  and the last known assignment was  $k \neq j$ . Note that this definition of ID switches is more similar to [33] and stricter than the original one [47]. Also note that, while it is certainly desirable to keep the number of ID switches low, their absolute number alone is not always expressive to assess the overall performance, but should rather be considered in relation to the number of recovered target. The intuition is that a method that finds twice as many trajectories will almost certainly produce more identity switches. For that reason, we also state the relative number of ID switches, which is computed as IDSW /

Recall.

These relationships are illustrated in Fig. 9. For simplicity, we plot ground truth trajectories with dashed curves, and the tracker output with solid ones, where the color represents a unique target ID. The grey areas indicate the matching threshold (see next section). Each true target that has been successfully recovered in one particular frame is represented with a filled black dot with a stroke color corresponding to its matched hypothesis. False positives and false negatives are plotted as empty circles. See figure caption for more details.

After determining true matches and establishing the correspondences it is now possible to compute the metrics. We do so by concatenating all test sequences and evaluating on the entire benchmark. This is in general more meaningful instead of averaging per-sequences figures due to the large variation in the number of targets.

### 5.2.2 Distance measure

To determine how close a tracker hypothesis is to the actual target, we will distinguish two cases as described below (see also Fig. 10).

**2D.** In the most general case, the relationship between ground truth objects and a tracker output is established

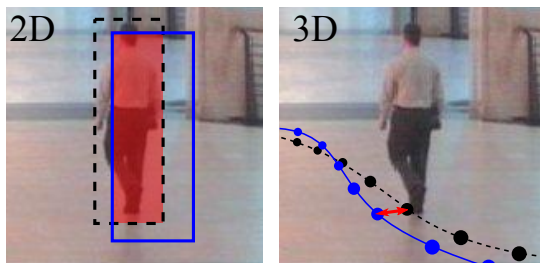


Fig. 10: The closeness between the tracker output (blue) and the true location of a target (black dashed) can be computed as a bounding box overlap or as Euclidean distance in world coordinates.

using bounding boxes on the image plane. Similar to object detection [19], the intersection over union (a.k.a. the Jaccard index) is usually employed as the similarity criterion, while the threshold  $t_d$  is set to 0.5 or 50%.

**3D.** When both locations, that of the tracker and that of the ground truth, are available as points in world coordinates, it is more sensible to directly compute the performance in 3D. To that end,  $d$  simply corresponds to the Euclidean distance and  $t_d$  is set to 1 meter for pedestrian tracking.

### 5.2.3 Multiple Object Tracking Accuracy

The MOTA [47] is perhaps the most widely used figure to evaluate a tracker’s performance. The main reason for this is its expressiveness as it combines three sources of errors defined above:

$$\text{MOTA} = 1 - \frac{\sum_t (\text{FN}_t + \text{FP}_t + \text{IDSW}_t)}{\sum_t \text{GT}_t}, \quad (1)$$

where  $t$  is the frame index and  $\text{GT}$  is the number of ground truth objects. We report the percentage MOTA  $(-\infty, 100]$  in our benchmark. Note that MOTA can also be negative in cases where the number of errors made by the tracker exceeds the number of all objects in the scene.

Even though the MOTA score gives a good indication of the overall performance, it is highly debatable whether this number alone can serve as a single performance measure.

**Robustness.** One incentive behind compiling this benchmark was to reduce dataset bias by keeping the data as diverse as possible. The main motivation is to challenge state-of-the-art approaches and analyze their performance in unconstrained environments and on unseen data. Our experience shows that most methods can be heavily overfitted on one particular dataset, but are not general enough to handle an entirely different setting without a major change in parameters or even in the model.

To indicate the robustness of each tracker over *all* benchmark sequences, we show the standard deviation on their MOTA score.

### 5.2.4 Multiple Object Tracking Precision

The Multiple Object Tracking Precision is the average dissimilarity between all true positives and their corresponding ground truth targets. For bounding box overlap, this is computed as

$$\text{MOTP} = \frac{\sum_{t,i} d_{t,i}}{\sum_t c_t}, \quad (2)$$

where  $c_t$  denotes the number of matches in frame  $t$  and  $d_{t,i}$  is the bounding box overlap of target  $i$  with its assigned ground truth object. MOTP thereby gives the average overlap between all correctly matched hypotheses and their respective objects and ranges between  $t_d := 50\%$  and  $100\%$ .

It is important to point out that MOTP is a measure of localization precision, *not* to be confused with the *positive predictive value* or *relevance* in the context of precision / recall curves used, *e.g.*, in object detection.

As we can see in Tab. 3, MOTP shows a remarkably low variation across different methods ranging between 69.6% and 71.6%. The main reason for this is that this localization measure is primarily dominated by the detections and the annotations and is less influenced by the actual tracker output.

If computed in 3D, the definition changes slightly to

$$\text{MOTP}_{3\text{D}} = 1 - \frac{\sum_{t,i} d_{t,i}}{t_d \cdot \sum_t c_t}. \quad (3)$$

Note that here it is normalized to be between 0 and 100%.

### 5.2.5 Track quality measures

Each ground truth trajectory can be classified as mostly tracked (MT), partially tracked (PT), and mostly lost (ML). This is done based on how much of the trajectory is recovered by the tracking algorithm. A target is mostly tracked if it is successfully tracked for at least 80% of its life span. Note that it is irrelevant for this measure whether the ID remains the same throughout the track. If a track is only recovered for less than 20% of its total length, it is said to be mostly lost (ML). All other tracks are partially tracked. A higher number of MT and few ML is desirable. We report MT and ML as a ratio of mostly tracked and mostly lost targets to the total number of ground truth trajectories.

In certain situations one might be interested in obtaining long, persistent tracks without gaps of untracked periods. To that end, the number of track fragmentations (FM) counts how many times a ground truth trajectory is interrupted (untracked). In other words, a fragmentation is counted each time a trajectory changes its status from tracked to untracked and tracking of that same trajectory is resumed at a later point. Similarly to the ID switch ratio (*cf.* Sec. 5.2.1), we also provide the relative number of fragmentations as  $\text{FM} / \text{Recall}$ .

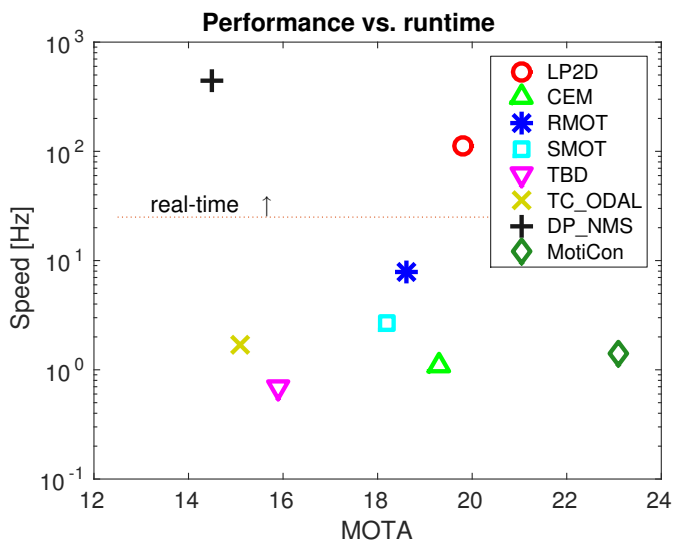


Fig. 11: Each marker represents a tracker’s performance measured by MOTA ( $x$ -axis) and its speed measured in frames per second (FPS) [Hz], *i.e.* higher and more right is better. Real-time ability is assumed at 25 FPS.

### 5.2.6 Runtime

Most research in multi-target tracking focuses on pushing the performance towards more accurate results with fewer errors. However, from the practical point of view, a method should be able to compute the results in a reasonable time frame. Of course, ‘reasonable’ varies depending on the application. Autonomous vehicles or tasks in robotics would require real-time functionality; surveillance assistance may tolerate a certain delay, while long-term video analysis may allow even much longer processing times. We demonstrate the relationship between tracker accuracy and speed in Fig. 11. As we can see, the fastest approach, DP\_NMS, performs worse on average while the baseline LP2D provides a good balance between speed and performance.

Note that accurately measuring the efficiency of each method is not straightforward. All baselines from Sec. 4 were executed on the same hardware (2.6 GHz  $\times$  16 cores CPU, 32 GB RAM) and the reported numbers do not include the detector’s time. For all submitted results we cannot verify the efficiency ourselves and therefore report the runtime as specified by the respective user.

### 5.2.7 Tracker ranking

As we have seen in this section, there are a number of reasonable performance measures to assess the quality of a tracking system, which makes it rather difficult to reduce the evaluation to one single number. To nevertheless give an intuition on how each tracker performs compared to its competitors, we compute and show the average rank for each one by ranking all trackers according to each metric and then averaging across all ten performance measures. Interestingly, the average rank roughly corresponds to the MOTA ordering, which

indicates that the tracking accuracy is a good approximation of the overall tracker performance.

## 6 CONCLUSION AND FUTURE WORK

We have presented a novel platform for evaluating multi-target tracking approaches. Our centralized benchmark consists of both existing public videos as well as new challenging sequences and is open for new submissions. We believe that this will enable a fairer comparison and guide research towards developing more generic methods that perform well in unconstrained environments and on unseen data.

In future, we will work on the standardization of the annotations for all sequences, continue our workshops and challenges series, and also introduce various other (sub-)benchmarks to welcome researchers and practitioners from other disciplines.

## REFERENCES

- [1] Reconstruction meets recognition challenge, <http://ttic.uchicago.edu/~rurtasun/rmrc/index.php>.
- [2] 1st workshop on benchmarking multi-target tracking, <http://www.igp.ethz.ch/photogrammetry/bmtt2015/home.html>.
- [3] Gurobi library, [www.gurobi.com](http://www.gurobi.com).
- [4] A. Alahi, V. Ramanathan, , and L. Fei-Fei. Socially-aware large-scale crowd forecasting. *CVPR*, 2014.
- [5] M. Andriluka, S. Roth, and B. Schiele. Monocular 3D pose estimation and tracking by detection. In *CVPR 2010*.
- [6] M. Andriluka, S. Roth, and B. Schiele. People-tracking-by-detection and people-detection-by-tracking. In *CVPR 2008*.
- [7] A. Andriyenko and K. Schindler. Multi-target tracking by continuous energy minimization. In *CVPR 2011*, pages 1265–1272.
- [8] S.-H. Bae and K.-J. Yoon. Robust online multi-object tracking based on tracklet confidence and online discriminative appearance learning. In *CVPR 2014*.
- [9] S. Baker, D. Scharstein, J. P. Lewis, S. Roth, M. J. Black, and R. Szeliski. A database and evaluation methodology for optical flow. *IJCV*, 92(1):1–31, Mar. 2011.
- [10] B. Benfold and I. Reid. Stable multi-target tracking in real-time surveillance video. In *CVPR 2011*.
- [11] J. Berclaz, F. Fleuret, E. Türetken, and P. Fua. Multiple object tracking using  $k$ -shortest paths optimization. *TPAMI*, 2011.
- [12] K. Bernardin and R. Stiefelhagen. Evaluating multiple object tracking performance: The CLEAR MOT metrics. *Image and Video Processing*, 2008(1):1–10, May 2008.
- [13] A. A. Butt and R. T. Collins. Multi-target tracking by Lagrangian relaxation to min-cost network flow. In *CVPR 2013*.
- [14] N. Dalal and B. Triggs. Histograms of oriented gradients for human detection. In *CVPR 2005*, pages 886–893.
- [15] C. Dicle, M. Sznaiar, and O. Camps. The way they move: Tracking multiple targets with similar appearance. In *ICCV 2013*.
- [16] P. Dollár, R. Appel, S. Belongie, and P. Perona. Fast feature pyramids for object detection. *PAMI*, 36(8):1532–1545, 2014.
- [17] P. Dollár, C. Wojek, B. Schiele, and P. Perona. Pedestrian detection: A benchmark. *CVPR*, 2009.
- [18] A. Ess, B. Leibe, K. Schindler, and L. Van Gool. A mobile vision system for robust multi-person tracking. In *CVPR 2008*.
- [19] M. Everingham, L. Van Gool, C. Williams, J. Winn, and A. Zisserman. *The PASCAL Visual Object Classes Challenge 2012 (VOC2012) Results*. 2012.
- [20] J. Ferryman and A. Ellis. PETS2010: Dataset and challenge. In *Advanced Video and Signal Based Surveillance (AVSS)*, 2010.
- [21] A. Geiger, M. Lauer, C. Wojek, C. Stiller, and R. Urtasun. 3d traffic scene understanding from movable platforms. *PAMI*, 2014.
- [22] A. Geiger, P. Lenz, and R. Urtasun. Are we ready for autonomous driving? The KITTI Vision Benchmark Suite. In *CVPR 2012*.
- [23] D. Helbing and P. Molnár. Social force model for pedestrian dynamics. *Physical Review E*, 51:4282, 1995.
- [24] J. a. Henriques, R. Caseiro, and J. Batista. Globally optimal solution to multi-object tracking with merged measurements. In *ICCV 2011*.

- [25] G. Huang, M. Ramesh, and T. B. B. Learned-Miller. Labeled face in the wild: a datadata for studying face recognition in unconstrained environments. Technical Report 07-49, University of Massachusetts, Amherst, 2007.
- [26] A. Johansson, D. Helbing, and P. Shukla. Specification of a microscopic pedestrian model by evolutionary adjustment to video tracking data. *Advances in complex systems*, 2007.
- [27] R. Kasturi, D. Goldgof, P. Soundararajan, V. Manohar, J. Garofolo, M. Boonstra, V. Korzhova, and J. Zhang. Framework for performance evaluation for face, text and vehicle detection and tracking in video: data, metrics, and protocol. *TPAMI*, 31(2), 2009.
- [28] M. Kristan et al. The visual object tracking vot2014 challenge results. *European Conference on Computer Vision Workshops (ECCVW). Visual Object Tracking Challenge Workshop*, 2014.
- [29] L. Leal-Taixé, M. Fenzi, A. Kuznetsova, B. Rosenhahn, and S. Savarese. Learning an image-based motion context for multiple people tracking. *CVPR*, 2014.
- [30] L. Leal-Taixé, G. Pons-Moll, and B. Rosenhahn. Everybody needs somebody: Modeling social and grouping behavior on a linear programming multiple people tracker. In *IEEE International Conference on Computer Vision Workshops (ICCV Workshops)*, pages 120–127, Nov. 2011.
- [31] L. Leal-Taixé, G. Pons-Moll, and B. Rosenhahn. Branch-and-price global optimization for multi-view multi-object tracking. *CVPR*, 2012.
- [32] K. Li, E. Miller, M. Chen, T. Kanade, L. Weiss, and P. Campbell. Cell population tracking and lineage construction with spatiotemporal context. *Medical Image Analysis*, 12(5):546–566, October 2008.
- [33] Y. Li, C. Huang, and R. Nevatia. Learning to associate: Hybrid-boosted multi-target tracker for crowded scene. In *CVPR 2009*.
- [34] J. Liu, P. Carr, R. T. Collins, and Y. Liu. Tracking sports players with context-conditioned motion models. In *CVPR 2013*, pages 1830–1837.
- [35] M. Mathias, R. Benenson, M. Pedersoli, and L. V. Gool. Face detection without bells and whistles. In *ECCV 2014*, 2014.
- [36] A. Milan, S. Roth, and K. Schindler. Continuous energy minimization for multitarget tracking. *PAMI*, 36(1):58–72, 2014.
- [37] A. Milan, K. Schindler, and S. Roth. Challenges of ground truth evaluation of multi-target tracking. In *2013 IEEE Conference on Computer Vision and Pattern Recognition Workshops (CVPRW)*, pages 735–742, June 2013.
- [38] K. Okuma, A. Taleghani, N. D. Freitas, J. J. Little, and D. G. Lowe. A boosted particle filter: Multitarget detection and tracking. *ECCV*, 2004.
- [39] S. Pellegrini, A. Ess, K. Schindler, and L. van Gool. You’ll never walk alone: Modeling social behavior for multi-target tracking. In *ICCV 2009*, pages 261–268.
- [40] S. Pellegrini, A. Ess, K. Schindler, and L. van Gool. You’ll never walk alone: modeling social behavior for multi-target tracking. *ICCV*, 2009.
- [41] H. Pirsivash, D. Ramanan, and C. C. Fowlkes. Globally-optimal greedy algorithms for tracking a variable number of objects. In *CVPR 2011*.
- [42] O. Russakovsky, J. Deng, H. Su, J. Krause, S. Satheesh, S. Ma, Z. Huang, A. Karpathy, A. Khosla, M. Bernstein, A. C. Berg, and L. Fei-Fei. *ImageNet Large Scale Visual Recognition Challenge*. 2014.
- [43] D. Scharstein and R. Szeliski. A taxonomy and evaluation of dense two-frame stereo correspondence algorithms. *IJCV*, 47(1-3):7–42, Apr. 2002.
- [44] D. Schuhmacher, B.-T. Vo, and B.-N. Vo. A consistent metric for performance evaluation of multi-object filters. *IEEE Transactions on Signal Processing*, 56(8):3447–3457, Aug. 2008.
- [45] S. M. Seitz, B. Curless, J. Diebel, D. Scharstein, and R. Szeliski. A comparison and evaluation of multi-view stereo reconstruction algorithms. In *CVPR 2006*, pages 519–528.
- [46] K. Smith, D. Gatica-Perez, J.-M. Odobez, and S. Ba. Evaluating multi-object tracking. In *Workshop on Empirical Evaluation Methods in Computer Vision (EEMCV)*.
- [47] R. Stiefelhagen, K. Bernardin, R. Bowers, J. S. Garofolo, D. Mostefa, and P. Soundararajan. The clear 2006 evaluation. In *CLEAR*, 2006.
- [48] A. Torralba and A. Efros. Unbiased look at dataset bias. In *CVPR 2011*.
- [49] C. Vondrick, D. Patterson, and D. Ramanan. Efficiently scaling up crowdsourced video annotation. *IJCV*, 101(1):184–204, Jan. 2013.
- [50] B. Wang, G. Wang, K. L. Chan, and L. Wang. Tracklet association with online target-specific metric learning. In *CVPR 2014*, June 2014.
- [51] L. Wen, W. Li, J. Yan, Z. Lei, D. Yi, and S. Z. Li. Multiple target tracking based on undirected hierarchical relation hypergraph. In *CVPR 2014*.
- [52] B. Wu and R. Nevatia. Tracking of multiple, partially occluded humans based on static body part detection. In *CVPR 2006*, pages 951–958, 2006.
- [53] Z. Wu, N. I. Hristov, T. L. Hedrick, T. H. Kunz, and M. Betke. Tracking a large number of objects from multiple views. *ICCV*, 2009.
- [54] J. Yoon, H. Yang, J. Lim, and K. Yoon. Bayesian multi-object tracking using motion context from multiple objects. *IEEE Winter Conference on Applications of Computer Vision (WACV)*, 2015.
- [55] A. R. Zamir, A. Dehghan, and M. Shah. GMCP-Tracker: Global multi-object tracking using generalized minimum clique graphs. In *ECCV 2012*, volume 2, pages 343–356.
- [56] H. Zhang, A. Geiger, and R. Urtasun. Understanding high-level semantics by modeling traffic patterns. In *ICCV 2013*.
- [57] L. Zhang, Y. Li, and R. Nevatia. Global data association for multi-object tracking using network flows. In *CVPR 2008*.